15

Self-field of a Hall probe and its effect on the parameters of objects under study

© Kh.R. Rostami, I.P. Nikitin

Fryazino Branch, Kotel'nikov Institute of Radio Engineering and Electronics, Russian Academy of Sciences, Fryazino, Moscow oblast, Russia
E-mail: rostami@ms.ire.rssi.ru

Received July 29, 2025
Revised January 20, 2026
Accepted January 20, 2026

Attention is drawn to the effect of the self-field $\mathbf{H}_{HT}$ of bias current $\mathbf{I}_{HT}$ through a Hall transducer (HT) on the objects of study and the measurement accuracy of the Hall magnetometer. The field $\mathbf{H}_{HT}$ of n-InSb$-i$-GaAs heteroepitaxial HT is considered. It is found that the force lines of the induction of $\mathbf{H}_{HT}$ undergo a stepwise change in their direction at the edges of a thin epitaxial n-InSb film. In the case of nonuniform distribution of IHT over the cross section of the film, these jumps create a voltage across the Hall contacts due to the anisotropy, growth-induced defects, and noneqipotentiality of the Hall contacts, thus leading to measurement error. Exact compensation of $\mathbf{H}_{HT}$ by the field of a current in antiphase to $\mathbf{I}_{HT}$ makes it possible not only to eliminate the effect of the self-field on the objects of study but also to lower the detection threshold of the magnetometer from $\sim 2.5 \cdot 10^{-7}$ to $\sim 5.75 \cdot 10^{-9}$ T in the range of fields from $2.5 \cdot 10^{-9}$ to $5 \cdot 10^{-7}$ T and temperatures from 77.4 to 150 K.

Keywords: Hall effect, heteroepitaxial structure, self-field, antiphase current, high-temperature superconductors.

DOI: 10.61011/TPL.2026.05.63287.20457

It is known [1,2] that the Hall voltage V_{HV} occurs in the ideal Hall transducer (HT) (symmetric design, homogeneous material, absence of side effects, etc.) when the bias current $\mathbf{I}_{HT}$ is passed through a thin high-resistance semiconductor plate with the width a, length l and thickness d in a magnetic field with induction of $\mathbf{B}_\perp$ perpendicular to the plate surface, on transverse Hall contacts placed in the center on each side:

$$V_{HV} = a/E_{HV} = a/J_{HT}R_{HT}B_\perp = R_{HT}B_\perp I_{HT}/d, \qquad (1)$$

where R_{HT} is the Hall coefficient, which doesn't depend on $B_\perp$ in weak magnetic fields and is only defined by semiconductor properties, E_{HV} is the Hall field strength, and $J_{HT} = I_{HT}/ad$ is the density of bias current through HT. In the semiconductor plate with predominant concentration of electrons $R_{HT} = (en)^{-1}$, where n and e are electron concentration and charge, respectively. Magnetic sensitivity of HT is calculated as

$$\gamma = \left|V_{HV}\right|(B_\perp)^{-1} = \left|R_{HT}\right|I_{HT}d^{-1} = I_{HT}(e\,n\,d)^{-1} = \left[Pa\mu_e(d\,l\,e\,n)^{-1}\right]^{1/2}, \qquad (2)$$

where P is the power dissipated at HT, and μ_e is the electron mobility. As can be seen from equation (2), for wide, short and thin HT plates, the higher mobility and the smaller the electron concentration are, the higher the magnetic sensitivity γ is. According to a large body of literature, indium antimonide has a higher μ_e and the lowest n among all known semiconductors, and indium antimonide HTs demonstrate more stable characteristics in a wide range of temperature and magnetic fields. The effect of self-field $\mathbf{H}_{HT}$ of $\mathbf{I}_{HT}$ through HT on the objects of interest was also reported in some studies. However, a detailed analysis of this problem hasn't been carried out, therefore evaluation of the effect of $\mathbf{H}_{HT}$ on magnetic-spatial resolution, linearity and accuracy of HT is still a challenging problem. To increase the magnetometer's spatial resolution, HT generally are placed near the surface of the test object and reduce the effective surface area of HT, and $\mathbf{I}_{HT}$ is reduced to decrease $\mathbf{H}_{HT}$. This leads to loss of sensitivity and performance, poor heat removal, high temperature drift of HT readings over time, low operation stability of such HT, and H_{HT}/I_{HT} remains on the same order of magnitude as that for HT with high $\mathbf{I}_{HT}$ and $\mathbf{H}_{HT}$. Consequently, to increase the magnetic-spatial resolution of any type of HT, $\mathbf{H}_{HT}$ of the used HT shall be initially compensated and HT shall be brought as close as possible to the surface of the test object, thus, simultaneously preventing the effect of HT on distribution of local fields around the test object and on its surface. $\mathbf{I}_{HT}$ of an ideal HT on wide and thin film can be visualized as a total current through parallel current threads with diameters equal to the film thickness: $I_{HT} = \sum I_{HTi}$. Currents $\mathbf{I}_{HTi}$ create solenoid fields $\mathbf{B}_{HTi}$ around them, while fields between threads compensate each other. Finally, for rectangular current threads, the fields $B_{HT} = \sum B_{HTi}$ on both sides of HT are homogeneous, parallel to the film surface and equal to each other.

Power lines $\mathbf{B}_{HT}$ form a loop around the HT current band. Differently directed power lines $\mathbf{B}_{HT}$ are perpendicular to the current through HT and parallel to the HT surface on both sides: $B_{HT3} = B_{HT}(-a/2, 0, -d/2)$ and $B_{HT4} = B_{HT}(a/2, 0, d/2)$. Moreover, since the film thick-

ness is considerably smaller than the film width, differently directed power lines on edges quickly change their direction on the film thickness scale: $B_{\mathrm{HT1}} = B_{\mathrm{HT}}(-a/2, 0, 0)$ and $B_{\mathrm{HT2}} = B_{\mathrm{HT}}(a/2, 0, 0)$, because $B_{\mathrm{HT3}}/B_{\mathrm{HT2}} = \mu_3/\mu_2$ on the film edges according to the boundary conditions. Here, μ_3 and μ_2 are permeabilities inside and on the edge of the film, respectively [3,4]. A picture is formed that is identical to a picture of power line concentration within the solenoid bore and power line divergence at the solenoid ends. In addition, the compensating field not only „presses" the power lines of $\mathbf{H}_{\mathrm{HT}}$ against the HT surface, but also moves the field away to the middle of the current band because $\mathbf{H}_{\mathrm{HT}}$ creates the Lorentz force that presses power lines against the surface and the middle of the film in case of unidirectional currents and, vice versa, moves them away in case of oppositely directed currents. Since [4] the force of interaction between two current bands is caused by components $\mathbf{B}_{\mathrm{HT}i}$ and perpendicular components $\mathbf{E}_{\mathrm{HT}i}$, distribution of power lines $\mathbf{B}_{\mathrm{HT}i}$ can be controlled by varying $\mathbf{E}_{\mathrm{HT}i}$. Since the field within cylindrical wire grows linearly from the center to the surface proportionally to the cylinder radius R, and decreases proportionally to $1/R$ [3–5] outside the cylinder, voltages on the Hall contacts V_{HT} can be set to zero and the influence of $\mathbf{H}_{\mathrm{HT}}$ on the test objects can be avoided simultaneously by controlling the compensating field amplitude and phase. Thus, the obtained result is very important to increase simultaneously both the spatial and magnetic resolutions of the Hall probe. Due to possible asymmetric arrangement of the Hall contacts, film material inhomogeneities and anisotropy, film growth defects, nonuniform distribution of the current density J_{HT} near the Hall contacts, etc., equation (1) is violated in real HTs as a result of variation of $I_{\mathrm{HT}} = dJ_{\mathrm{HT}}$ on the film edges. Consequently, jumps of $\mathbf{B}_{\mathrm{HT1}}$ and $\mathbf{B}_{\mathrm{HT2}}$ are different. This induces different shift of the current and equipotential lines near the Hall contacts, consequently the concentration of induction power lines $\mathbf{B}_{\mathrm{HT}}$ near the contacts will be different and $\mathbf{B}_{\mathrm{HT}}$, which is integral over the film area, becomes non-zero. Thus, in a zero external magnetic field, the average induction $\mathbf{B}_{\mathrm{HT}}$ over the film area of the nonuniform asymmetric self-field $\mathbf{H}_{\mathrm{HT}}$ induces additional voltage on the Hall contacts

$$V_{\mathrm{HT}} \sim R_{\mathrm{HT}} B_{\mathrm{HT}} I_{\mathrm{HT}}/d \sim R_{\mathrm{HT}} I_{\mathrm{HT}}^2/d. \tag{3}$$

In case of alternating current through HT, $I_{\mathrm{HT}} = I_0 \cos(\omega t)$,

$$V_{\mathrm{HT}} \sim (R_{\mathrm{HT}}/d) I_0^2 \cos^2(\omega t). \tag{4}$$

As can be seen from equations (3) and (4), the value of V_{HT} does not depend on the direction of I_{HT}. The value of B_{HT} can be determined using the vector

$$V_{\mathrm{HT}} \sim R_{\mathrm{HT}} B_{\mathrm{HT}} I_{\mathrm{HT}}/d \sim R_{\mathrm{HT}} I_{\mathrm{HT}}^2/d. \tag{3}$$

circulation theorem:

$$2Bl = \mu_0 i l. \tag{5}$$

Here, l is the length of the loop side parallel to the current carrying plane [4], and i is the linear current density consisting of current per unit length of the film cross-section. For points near the film surface and away from the film edges

$$B = \mu_0 i/2 = (\mu_0 I)/2a. \tag{6}$$

According to (6), for standard PHE603118B indium antimonide HT (NPF Sensor, Saint Petersburg) with a nominal current of $I_{\mathrm{HT}} = 100\,\mathrm{mA}$ and $50 \times 100\,\mu\mathrm{m}$ effective area [5] used for the purpose of this work, we have

$$B_{\mathrm{HT}} = \mu_0 i_{\mathrm{HT}}/2 = (\mu_0 I_{\mathrm{HT}})/2a \approx 10^{-4}\,\mathrm{T}. \tag{7}$$

I_{HT} on the Hall contacts induces the voltage

$$V = V_{\mathrm{HV}} + V_{res} + V_{\mathrm{HT}} + \Sigma V_i. \tag{8}$$

In this expression, V_{res} is the residual nonequipotentionality voltage that occurs on the HT's Hall contacts in the zero external magnetic field; ΣV_i is the total bias voltage (thermomagnetic voltage induced by temperature effects and temperature dependence of the Hall coefficient) [1]. According to the datasheet [5], conversion factor γ of the PHE603118B HT is $> 50\,\mu\mathrm{V}/10^{-3}\,\mathrm{T}$, $V_{res} < 50\,\mu\mathrm{V}$, temperature coefficient of residual voltage is $< 0.01\,\mu\mathrm{V}/^{\circ}\mathrm{C}$, temperature coefficient of sensitivity is $< 2\,\%/^{\circ}\mathrm{C}$. According to equation (4)

$$V_{\mathrm{HT}} \sim (R_{\mathrm{HT}}/d) I_0^2 (1 + \cos 2\omega t)/2, \tag{9}$$

voltage on the Hall contacts induced by the self field H_{HT} contains a constant components and a variable with the second harmonic frequency. Therefore, according to (7), the magnetometer output signal at $B_{\mathrm{HT}} \approx 10^{-4}\,\mathrm{T}$ in the zero external field induces $V_{\mathrm{HT}} \approx 10\,\mu\mathrm{V}$ on the Hall contacts, therefore, as shown in [6], magnetic sensitivity of the magnetometer without HT compensation is max. $2.5 \cdot 10^{-7}\,\mathrm{T}$. Thermal noise ΣV_i can be significantly reduced due to operation in isothermal conditions: HT was kept in liquid nitrogen or in a gas-flow microcryostat at a temperature set with an accuracy of 0.01 K. Thus, in the zero external magnetic field, V_{res} and V_{HT} make the main contribution to equation (8).

To reduce the measurement error caused by the effect of $\mathbf{H}_{\mathrm{HT}}$ on HT readings and physical parameters of the test object, $\mathbf{H}_{\mathrm{HT}}$ was thoroughly compensated. Two identical HTs with similar specifications were used for this. A secondary HT used for compensation of $\mathbf{H}_{\mathrm{HT}}$ was placed on the back side of the primary HT substrate. Both HTs were placed strictly parallel to each other into a recess in a fixed copper disc mounted on the lower load-bearing part of the magnetic field sensor. Then, current was passed through the secondary HT opposite in phase to $\mathbf{I}_{\mathrm{HT}}$ of the primary HT. Magnetometer sensitivity was increased from $\sim 2.5 \cdot 10^{-7}$ to $\sim 5.75 \cdot 10^{-9}\,\mathrm{T}$ at 19 Hz by adjusting the amplitude and phase using a phase shifter and synchronous detection. At higher frequencies, phase difference between I_{HT} and $V_{\mathrm{HV}}(B)$ increases, the shape of $V_{\mathrm{HV}}(B)$ changes

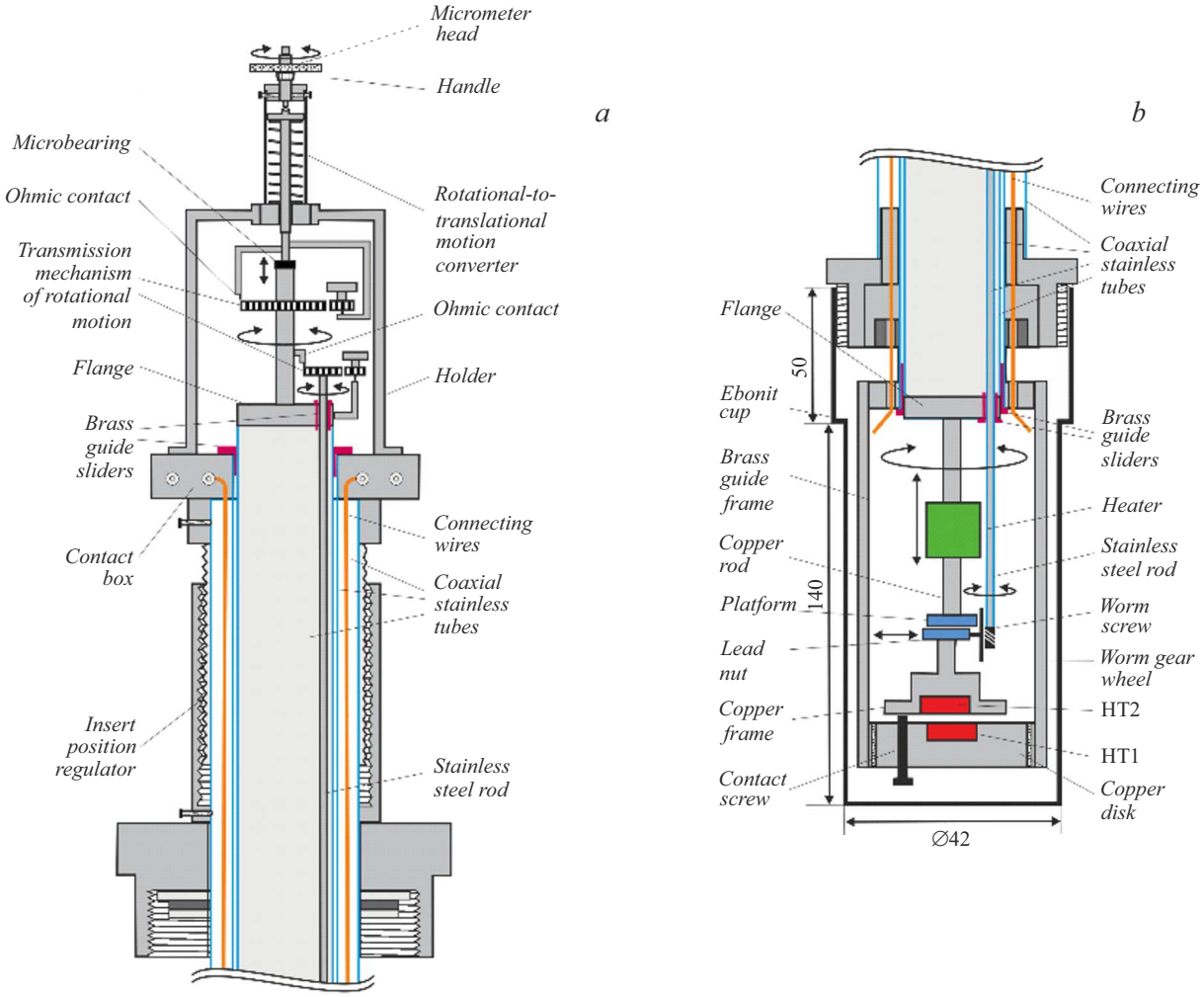

Figure 1. Measurement setup.

and preliminary compensation of both the first and second harmonics of $V_{\mathrm{HV}}(B)$ gets more complicated. All these factors have high effect in case of weak magnetic fields and reduce the accuracy of field measurement. In addition, exclusion of the second harmonic is very important for spectroscopy of the measured signal by harmonics.

To study the spatial distribution of $\mathbf{H}_{\mathrm{HT}}$ on the surface and around HT, a system has been developed to move test HT2 along the Z axis at a distance up to 25 mm with an accuracy of $\sim 1\,\mu$m, rotate HT2 on its axis at $\varphi = 360^\circ$ with an accuracy of 2°, and to move it along the X axis at a distance up to 5 mm with respect to measurement HT1 with an accuracy of $\sim 1\,\mu$m.

Figure 1 shows the top (a) and bottom (b) of the experimental system. Topology of $\mathbf{B}_{\mathrm{HT}}(\varphi, X, Z)$ was probed by moving test HT2 noncompensated for $\mathbf{H}_{\mathrm{HT}}$ relative to the surface of measurement HT1 compensated for $\mathbf{H}_{\mathrm{HT}}$. For this, $\mathbf{B}_{\mathrm{HT}}$ was first measured on one of the Hall contacts and then its variation was measured along the line connecting this Hall contact with the Hall contact on the opposite side of HT2 along the X axis using a translational table. In this case, the line connecting the HT2 Hall contacts coincided with the line connecting the HT1 Hall contacts, i. e. the angles at ends of these lines were $\varphi_1 = 0^\circ$ and $\varphi_2 = 180^\circ$. By alternately changing the X and Z coordinates and by rotating HT2 at the angle φ on its axis that coincides with the axis passing through the geometrical center of HT1, distribution of B_{HT} on the HT2 surface was mapped by means of HT1.

Investigations were performed in FC (field cooling) and ZFC (zero field cooling) modes [6,7] on high-temperature superconducting (HTSC) samples with different sizes, structures, critical superconducting transition temperature T_c, superconducting transition width ΔT_c, critical current densities J_c, first critical magnetic fields H_{c1}, maximum densities $B_{tr}^{\max}(0)$ of the trapped magnetic flux (TMF) in the center of sample surfaces. The samples included $YBa_2Cu_3O_{7-x}$ (YBCO)single crystals (sample No. 1); $Bi_2Sr_2CaCu_2O_{8+x}$ single crystals (sample No 2), bulk textured (the c axis is perpendicular to the sample plane) YBCO quasi-single-

Properties of samples and measurements

Sample No.	Size, mm	T_c, K	ΔT_c, K	J_c, A/cm^2	H_{c1}, 10^{-4} T	$B_{tr}^{\max}(0)$, 10^{-5} T ($Z=0.01$–1 mm)		V_{oput}, μV ($Z=0.01$–1 mm)	
						ZFC	FC	ZFC	FC
1	$\sim 1\times 1\times 0.05$	~ 91	~ 0.6	$\sim 5.3\cdot 10^5$	~ 50	~ 0; 1.2	~ 0; 2.2	~ 1; 3.2	~ 1; 2.2
2	$\sim 4\times 4\times 0.1$	~ 90.2	~ 0.6	$\sim 7.9\cdot 10^4$	~ 5.2	~ 1; 3.2	~ 1; 3.5	~ 2; 2.6	~ 3.5; 5.1
3	$\sim (6-8)\times 0.7$	~ 92	~ 1	$\sim 2.4\cdot 10^3$	~ 3.3	~ 0; 0	~ 2; 4.6	~ 3.5; 3.1	~ 6.5; 11
4	$\sim (6-8)\times 2.1$	~ 92	~ 1	$\sim 1.3\cdot 10^3$	~ 0.8	~ 0; 0.5	~ 3.5; 6.1	~ 3.9; 4.6	~ 9.4; 15
5	$\sim (6-8)\times 4.3$	~ 92	~ 1	$\sim 1.4\cdot 10^2$	~ 0.1	~ 1; 0.8	~ 5.9; 12.8	~ 5.6; 6.3	~ 12.7; 18
6	$\sim 10\times 10\times (0.0004-0.001)$	~ 92	~ 0.6	$\sim 6.8\cdot 10^5$	~ 35	~ 0; 0	~ 3.5; 5.1	~ 3.8; 4.2	~ 2.5; 8.1

crystal samples (No. 3), polycrystalline samples textured along the c axis (No 4), non-textured ceramic HTSC YBCO samples (No. 5) and epitaxial YBCO films with the c axis perpendicular to the $NdGaO_3$ (110) substrate plane (No. 6).

The following experiments were performed to estimate the degree of compensation of $V_{\rm HT}$ induced in $\mathbf{H}_{\rm HT}$.

Initially without compensation of $\mathbf{H}_{\rm HT}$, the YBCO sample was brought to HT1 along the Z axis in the ZFC mode. It has been found that, due to diamagnetic shielding, an increase in J_c and H_{c1} caused a decrease in the out-of-balance signal at the magnetometer output. When the sample was taken away from HT1, the out-of-balance signal returned to its initial value, and the sample was again brought to the HT1 surface, the out-of-balance signal increased. Then, the HTSC YBCO sample near HT1 was heated to a temperature above T_c and cooled down again to the liquid nitrogen temperature $T = 77.4$ K in the FC mode. This experiment detected an even greater increase in the out-of-balance signal at the magnetometer output compared with the ZFC mode where the sample in the superconducting state was brought to the HT1 surface. When the YBCO sample was removed from the HT1 surface, as in the first experiment, the out-of-balance signal decreased and took on its initial value. In the ZFC mode, variation of the magnetometer output signal was caused by demagnetization fields of the YBCO sample, which were induced by $\mathbf{H}_{\rm HT}$ [6]. In the FC mode where the YBCO sample near the HT1 surface was cooled down from a temperature above T_c to 77.4 K, $\mathbf{H}_{\rm HT}$ penetrated the sample through weak Josephson couplings. When the sample was removed from the HT1 surface, magnetic flux was trapped in the sample by the field $\mathbf{H}_{\rm HT}$, and this caused an increase in the out-of-balance signal at the magnetometer output when the sample was brought again to the transducer surface. Properties of samples and measurements are given in the table. Similar results were also obtained when sample No. 1 was replaced with samples No 2–6. However, for sample No. 2, the out-of-balance signal at the magnetometer output increased due to a weak first critical magnetic field H_{c1} and a higher TMF density $B_{tr}^{\max}(0)$ compared with those of sample No. 1. For samples No 3–5 , the out-of-balance signal at the magnetometer output increased even more due to a lower H_{c1} and much higher $B_{tr}^{\max}(0)$ than those of samples No 1, 2, 6. As shown in the table, the results are highly distorted due to small dimensions of sample No 1, and this shall be kept in mind when testing small objects.

When a ferromagnetic film was brought to the HT1 surface, $\mathbf{H}_{\rm HT}$ was significantly strengthened (due to high film permeability), causing an increase in the out-of-balance signal by more than an order of magnitude. Therefore, it shall be kept in mind that, when magnetic concentrators with high permeability are used for strengthening and focusing the power lines of magnetic field induction on the HT surface [8], strengthening of HT's magnetic sensitivity as well as degradation of HT's spatial resolution are caused.

For the FC and ZFC modes, repeated experiment with compensated $H_{\rm HT}$ has detected that the magnetometer output voltage was not changed, when both superconducting and magnetic film was brought to the HT1 surface.

Figures 2 and 3 show 3D dependences $B_{\rm HT}(\varphi, X, Z)$ in cases when φ and X vary with pre-defined Z (Figure 2) and φ and Z vary with pre-defined X (Figure 3). It can be seen that the measured tangential and perpendicular components of $\mathbf{B}_{\rm HT}$ on the Hall contacts are equal to $\sim 1.34\cdot 10^{-4}$ and $-1\cdot 10^{-4}$ T, which adequately agrees in absolute magnitude with the estimated value of$\sim 10^{-4}$ T, calculated using equation (7). Thus, as seen from Figures 2 and 3, the topology of $_{\rm HT}$ distribution over the HT surface and around HT is very nonuniform. Therefore, it shall be kept in mind that interaction between $_{\rm HT}$ and local fields on the surface of the samples will result in significant distortion of three-dimensional distribution of such quantities as MFC density [8] on the surface of the HTSC samples and magnetization of magnetic materials [9,10].

It also follows from the findings that in order to achieve higher accuracy and to simplify the $_{\rm HT}$ compensation procedure, identical (with similar a, l, d and input resistance) epitaxial n-InSb thin films shall be grown during HT fabrication on both sides of the single-crystal semi-insulating i-GaAs substrate in a single process cycle. In addition, for investigating local fields of small objects, a balance of HT and object sizes shall be kept due to increasing impact of $\mathbf{H}_{\rm HT}$.

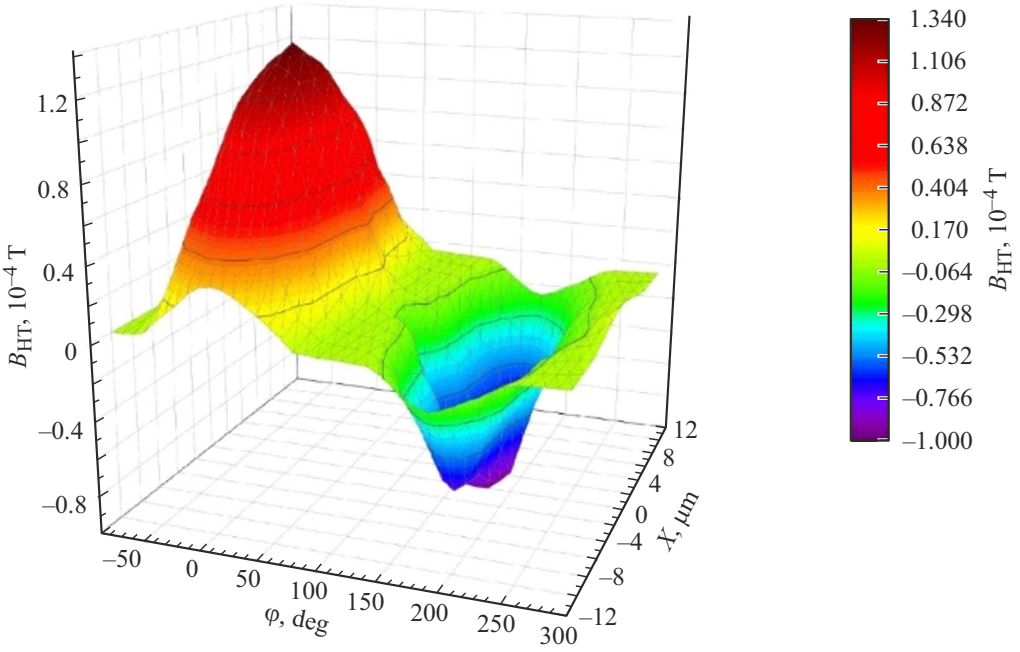

Figure 2. 3D dependences of $B_{HT}(\varphi, X, Z)$ in case when φ and X vary with the pre-defined Z.

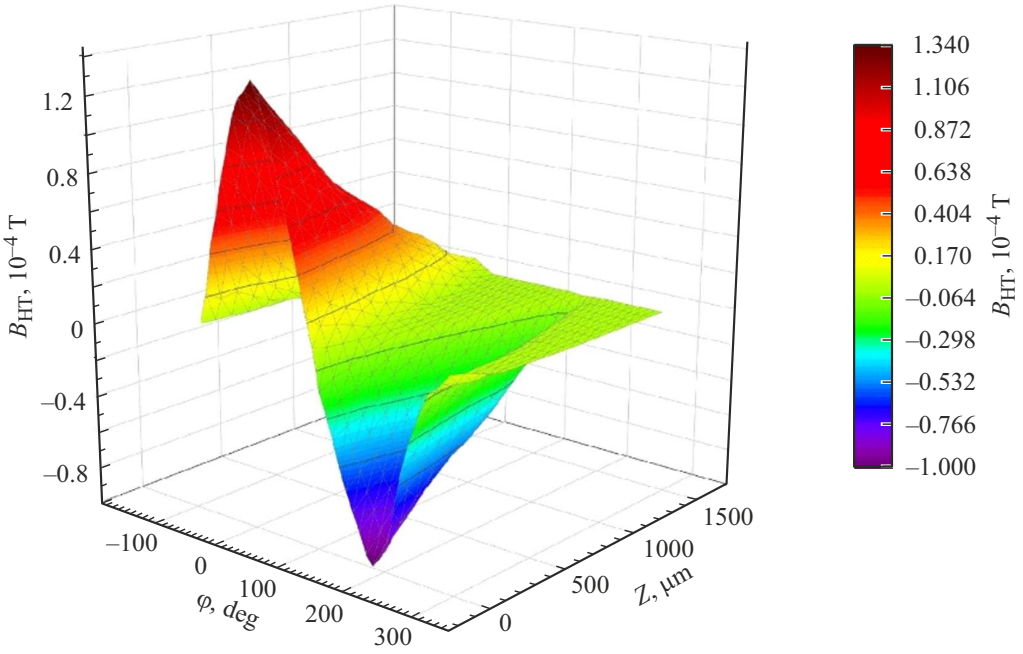

Figure 3. 3D dependences of $B_{HT}(\varphi, X, Z)$ in case when φ and Z vary with pre-defined X.

Funding

This study was carried out under state order No 075-00395-25-00 of Kotelnikov Institute of Radio Engineering and Electronics of the Russian Academy of Sciences.

Conflict of interest

The authors declare no conflict of interest.

References

[1] E.V. Kuchis. *Gal'vanomagnitnye effekty i metody ikh issledovaniya* (M., Radio i Svyaz', 1990) (in Russian).
[2] H.P. Baltes, R.S. Popović, Proc. IEEE, **74** (8), 1107 (1986). DOI: 10.1109/PROC.1986.13597
[3] A.V. Astakhov, Yu.M. Shirokov, *Kurs fiziki* (Glav. red. fiz.-mat. lit., M., 1980), t. 2. (in Russian)
[4] S.G. Kalashnikov. *Elektrichestvo* (Nauka, M., 1985) (in Russian).

[5] I.E. Irodov, *Elektromagnetizm. Osnovnye zakony* (Laboratoriya bazovykh znanii, M., 2002).(in Russian)
[6] *Preobrazovateli Kholla* [Elektronnyi resurs]. http://sensorspb.ru/price5.doc
[7] Kh.R. Rostami, I.P. Nikitin, Next Res., **2** (2), 100331 (2025). DOI: 10.1016/j.nexres.2025.100331
[8] Kh.R Rostami, Supercond. Sci. Technol., **36** (9), 095012 (2023). DOI: 10.1088/1361-6668/ace8c9
[9] R.S. Popovic, in *Proc. of the 2014 29th Int. Conf. on microeletronics (MIEL 2014)* (IEEE, 2014), p. 69–74. DOI: 10.1109/MIEL.2014.6842087
[10] V.K. Ignat'ev, A.A. Orlov, S.V. Perchenko, D.A. Stankevich, Tech. Phys. Lett., **43** (8), 687 (2017). DOI: 10.1134/S1063785017080090

Translated by E.Ilyinskaya